10.2478/v10063-010-0011-5

ANNALES
UNIVERSITATIS MARIAE CURIE-SKŁODOWSKA
LUBLIN – POLONIA

VOL. LXV, 11 SECTIO AA 2010

The influence of gold on the properties of silica mesoporous materials♣

W. Gac[1,a], S. Pasieczna-Patkowska[a] and L. Kępiński[b]
[a]*Department of Chemical Technology, University of Maria Curie-Skłodowska, Maria Curie-Sklodowska Sq. 3, 20-031 Lublin, Poland*
[b]*Institute of Low Temperature and Structure Research, PAS, Okólna 2, 55-422 Wrocław, Poland*

The properties of gold modified silica mesoporous materials were investigated on the successive preparation stages. Samples were obtained by the direct introduction of HAuCl4 aqueous solution to the synthesis mixture of silica. It was stated that partial substitution of -Cl with -OH ligands occurred in the diluted solutions of HAuCl4. The replacement of -Cl with -Br groups in gold complexes took place in the synthesis mixture containing hexadecyltrimethylammonium bromide surfactant molecules. It was found that gold species influenced the removal of organic templates from the channels of silica materials. Pore arrangement was not strongly distorted by the presence of small amounts of gold. Heat treatment led to the pronounced changes of the nature of gold species.

1. INTRODUCTION

The M41S family of the ordered silica mesoporous materials has found great interests in the last years [1-5]. Their unique features are the extraordinarily regular structure, very narrow pore size distribution, and a large surface area, often above 1000 m^2/g. The MCM-41 materials contain uniform, parallel pores of the size ranging from 2 to 5 nm. The modified silica mesoporous materials

♣This article is dedicated to Professor Tadeusz Borowiecki on the occasion of his 65th birthday

[1] Corresponding author: Wojciech Gac, tel. +48 081 5375526, Fax: +48 081 5375565, e-mail: Wojciech.Gac@umcs.lublin.pl

have been widely studied as adsorbents, optical materials, catalysts, and nanocasting devices. The application of the silica mesoporous materials for preparation of strongly dispersed metal crystallites is promising with regards of well regular structure and the presence of uniform pores.

Gold has been perceived for long time as an expensive, inert metal of high corrosion resistance and low catalytic activity. Nowadays, much of the worldwide gold production is consumed by the jewellery, while minor quantities are utilized in the industry, mainly in the electronics, and in the dentistry [6]. In 90^{th} of last century it was stated the small gold species may reveal unique properties. Gold nanoparticles show strong surface plasmon resonance effect and can be used as new materials of special optical properties, e.g. for drug delivery, cancer recognition, toxin detection or directly as the components of new-types of medicines [7,8]. Gold catalysts have been studied for about ten years in the large number of the environmental processes, synthesis of the important chemicals, and energy production systems [9-18].

Gold can be incorporated into the silica mesoporous materials by the different techniques. The isoelectric point (IEP) of pure silica materials is relatively low (at the level of 1–2) [19]. The direct impregnation method with the use of $AuCl_3$ or $HAuCl_4$ solution may fail due to in general negative charge of the surface of the silica support. Moreover, the attempts of the deposition of $[Au(OH)_nCl_{4-n}]^-$ or $Au(OH)_3$ gold species, formed at higher pH, e.g. via Na_2CO_3 addition or urea decomposition may lead to the dissolution of silica and structure disruption. Such problems have been partially solved by the adsorption of gold precursors after functionalisation of the silica surface, using amine groups, e.g. 3-amino-propyl-trimethoxysilane [20,21], thiol groups [22] or by the deposition of metal oxides, e.g. titania [23]. In another route, the sorption of gold on the negatively charged silica surface has been performed through a gold cationic complex precursor, e.g. $[Au(en)_2]^{3+}$ (en = ethylenediamine) [16]. Similar materials have been prepared by the gas-phase grafting using organo-gold complexes, e.g. acethylacetonate [24]. The interesting materials have been synthesized by the application of nanoparticles, by the direct addition to the synthesis mixture of the silica materials. The increase of the adsorption capability and increase of gold dispersion have been obtained by the direct introduction of amine compounds, e.g. quaternary ammonium ligands having triethoxysilyl terminal groups which stabilized gold nanoparticles [25].

Direct introduction of gold precursors to the synthesis mixture of silica materials is one of the simplest methods. Studies of the formation gold modified silica mesoporous materials by such method are still far from complete. The aim of our work was investigation of the formation of silica mesoporous materials modified with gold and identification of the most crucial preparation stages for

obtaining new optical materials and catalysts with precisely controlled structure, location and the size of gold species.

2. MATERIAL AND METHODS

2.1. Preparation of materials

Silica mesoporous materials were obtained by the modified procedures described in the literature [26].The changes of porosity of materials was achieved by the application of hexa- and octadecyltrimethylammonium bromide surfactants. The silica materials were prepared by dissolving 2 g of the surfactant in the 80 cm^3 of distilled water at 40^{o}C. Then 8 ml of tetraethylortosilicate (TEOS) was slowly introduced to the mixture while stirring. The pH of the solution was slowly increased by the introduction of 8 ml of ammonium hydroxide (25 wt. % solution). The mixture was stirred for 1 h at 40^{o}C. The obtained product was filtered, washed with distilled water, dried overnight at 90^{o}C and calcined in air at 550^{o}C for 6 hrs. Gold was introduced to the support in the initial stage of silica formation. Different amounts of 0.01 M $HAuCl_4$ solution were introduced to the mixture containing surfactant molecules (7 and 14 cm^3, respectively). The same amounts of TEOS and then ammonia as in the preparation of pure silica materials were added. The mixture was stirred for 1h at 40^{o}C. Pale-yellow precipitate was filtered, washed, and dried. The products with pink colour were obtained after calcination.

2.2. Characterization of the materials

The catalysts composition was determined by the X-ray fluorescence method (ED-XRF Canberra 1510, USA). The mesoporous structure of calcined materials was determined by the analysis of the nitrogen adsorption/desorption isotherms obtained volumetrically at -196^{o}C (77 K) using ASAP 2405N apparatus (Micromeritics Corp., USA). Before measurements the samples were outgassed (~10^{-2} Pa) at 220^{o}C. The adsorption data were used to evaluate BET specific surface area, S_{BET} (from the linear BET plots) [27]. The mesopore structure was characterized by the distribution function of mesopore volume calculated by applying the Barrett-Joyner-Halenda (BJH) method. Porous structure of the samples and the properties of gold crystallites after drying and calcination were investigated by the X-ray diffraction studies (XRD) performed in the HZG-4 diffractometer using CuK_α radiation. The primary mesopore diameter (w_d) was calculated from the XRD (100) interplanar spacing d using the following equation [28]:

$$w_d = cd\left(\frac{\rho V}{1+\rho V}\right)^{1/2}$$

where: c is a constant equal to 1.213 for cylindrical pores, ρ – is the pore wall density, assumed to be equal to that of amorphous silica – 2.2 g/cm^3, V – is the volume of the primary mesopores, calculated here by the BJH method from the adsorption branch of the isotherms.

Morphology and microstructure was investigated by the atomic force microscopy (AFM) NanoScope III (Digital Instruments) and the transmission electron microscopy (TEM) Philips CM-20 SuperTwin, operating at 200 kV and providing 0.25 nm resolution. The analysis of TEM images and FFT (Fast Fourier Transform) patterns was made with ImageJ program [29]. The specimens for TEM were prepared by dispersing some powder sample in methanol and putting a droplet of the suspension on a copper microscope grid covered with perforated carbon.

Raman spectra were recorded on the inVia Reflex Raman Microscope (Reinshaw,UK) with solid state laser operating at 514 nm in regular mode, and 2400 l/mm grating, using exposure time 10 s. To obtain better signal to noise ratio, up to 500 accumulations was taken.

FT-IR/PAS spectra of the samples were recorded by means of the Bio-Rad Excalibur 3000MX spectrometer equipped with photoacoustic detector MTEC300 (in helium atmosphere in a detector) over the 4000–400 cm^{-1} range at the resolution of 4 cm^{-1} and maximum source aperture. The spectra were normalized by computing the ratio of a sample spectrum to the spectrum of a MTEC carbon black standard. A stainless steel cup (diameter 10 mm) was filled with powder samples (thickness < 6 mm). Interferograms of 1024 scans were averaged for each spectrum.

The removal of the templates was investigated by the temperature programmed desorption technique using mass spectrometer HAL201RC (HIDEN Analytical). Samples (0.05 g) were placed inside the quartz reactor (i.d.=10 mm). Samples were initially washed with helium at room temperature for 1h and heated up to the 800^{o}C with the linear temperature increase. Light products were analyzed by the detection of the selected ions, including m/e = 2, 14, 16, 17, 18, 28, 30, 32, 44, 59, 96, respectively.

UV-Vis reflectance spectra were recorded by means of Specord M40 (Carl Zeiss, Jena, Germany) equipped with integration sphere. ZnO sample was used as the reference substance. The reflectance spectra were measured at 10 nm s^{-1} rate over 200–900 nm range with slit spectral width 1 nm.

3. RESULTS AND DISCUSSION

3.1. The properties of the synthesis mixture

Metal ionic species in the aqueous solution, containing surfactant molecules, such as octadecyltrimethylammonium bromide can be located around the organic

micelles as S^+I^- pairs or $S^+X^-I^+$ assemblies. Their presence may lead to the changes of the stability of micellar structure. The ionic species may modify the rate of silica condensation, introduce distortion, generate different silica structure. Gold species may locate in the framework or extraframework positions of the carrier [30]. Chloride ligands in the $[AuCl_4]^-$ complex anion, when pH of the solution is increased, can be replaced with hydroxyl groups, giving the variety of negative or neutral complexes with general formula $[Au(OH)_nCl_{4-n}]^-$ (where n = 0–4), including $Au(OH)_3$. Gold in the presence of ammonia may form positive complexes, such as $[Au(NH_3)_4]^{3+}$ or $[Au\ (NH_3)_2(OH)_2]^+$, which can be directly bounded to the "as prepared" silica walls [31]. Gold in the synthesis conditions can be also easily reduced to the metallic form, e.g. by the light, high temperature or chemical agents. Small metallic gold species can be stabilised by the ammonium groups of the surfactant molecules, via formation of N-donor complexes. On the other hand rapid reduction may lead to the uncontrolled growth of the metal species. Such processes may occur during wet synthesis, drying, and especially - high-temperature calcination stages, what will be further discussed.

The state of the $HAuCl_4$ complexes is strongly related to the pH of the solution. An increase of pH of the solution leads to the replacement of Cl^- wih OH^- groups [32]. We have confirmed that hydrolysis of chloroauric acid can take place in the dilute solutions. Figure 1 shows Raman spectra of the solutions with low concentration of $HAuCl_4$ (~0.001M), directly used in the synthesis of Au(I)-MCM-41 sample. There is visible weak peak located at 351 nm with shoulder at 330 nm. The planar $[AuCl_4]^-$ complex reveals two strong Au-Cl stretching vibrations. An increase of the pH of $HAuCl_4$ solution or decrease of gold concentration lead to the gradual decrease of the intensity of these vibrations, and simultaneously to the increase of the vibrations of the groups with maxima, located at around 570 nm. Such effects are ascribed to the partial substitution of Cl with OH groups, connected with Au-Cl and Au-OH stretching modes, respectively [32,33]. The dilute solution contains partially hydrolised gold complexes $[Au(OH)_nCl_{4-n}]^-$ (where n = 1–3). However detailed determination of the nature of the complexes in our studies was difficult due to very low concentration of gold.

In the solution of $HAuCl_4$ containing surfactant molecules, dissolved at 40°C, a typical Au-Cl vibrations are no longer visible (Figure 1a). This effect can be ascribed to the further replacement of Cl with OH, the replacement with Br groups, formation of Au-N type complexes with amine ligands or reduction and formation of gold nanoparticles stabilized with amine groups of surfactants. The first effect can be connected with a slight increase of pH of the solution upon ammine addition. It was recently demonstrated that hexadecyltrimethylamonium surfactants can be easily decomposed to trimethylamine or N,N-dimethyl-

hexadecylamine and hexadecanol during synthesis of MCM-41 materials [34]. Thus the solution may include the traces of different types of N-containing compounds, what increase the probability of the formation Au-N type complexes. The changes of the colour of the solution from week to deep yellow may supports the hypothesis of the partial reduction of Au(III) compounds. Octadecyltrimethylammonium bromide surfactant has been frequently used for the synthesis of gold nanoparticles [35,36]. Such compounds have been regarded as the protection agents, which prevented formation of large metallic species or influenced their shape. Moreover, the appearance of the strong maxima located at 195 and 214 cm^{-1} indicates the formation of $[AuBr_4]^-$ complex [38,39].

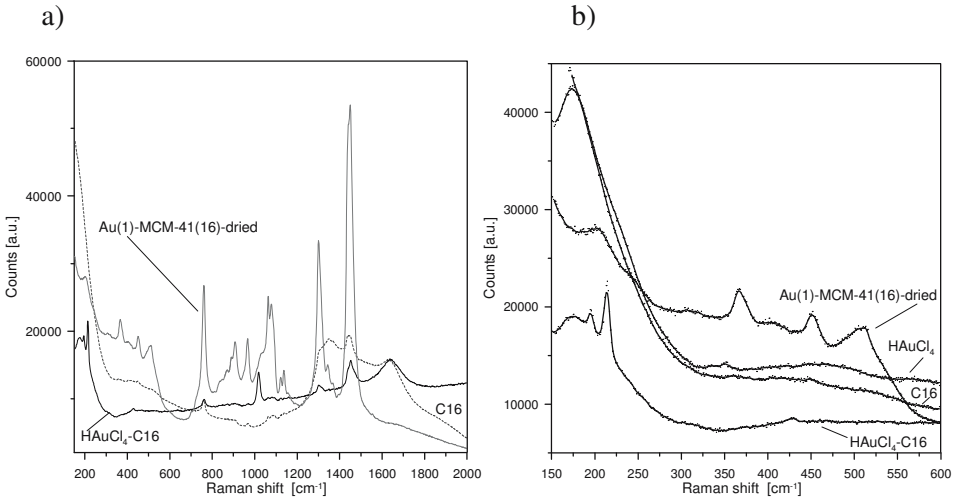

Fig. 1. Raman spectra of the solutions of hexadecyltrmethylammonium bromide (C16), ~0.001M $HAuCl_4$, mixture of $HAuCl_4$ and hexadecyltrmethylammonium bromide ($HAuCl_4$-C16), and dried sample of Au(1)-MCM-41(16); a) low, and b) wide range of vibrations.

The synthesis of the silica mesoporous materials has been a subject of extensive studies. It has been stated that the assembling of the surfactant molecules in the solution plays a crucial role in the development of the materials with regular and ordered pore systems. Figure 1b reveals Raman vibrations of CH groups of the surfactant molecules in the solution and in the solid sample of Au(1)-MCM-41(16) without washing nor drying. Well visible band located at 1450 cm^{-1} can be connected with scissoring mode of CH_2 groups, overlapped with the CH_3 asymmetric bending vibrations (1440 cm^{-1}). A strong maximum at 1300 cm^{-1} is attributed to the $-(CH)_2-$ in phase twisting mode, while the maxima in the range 1100–800 cm^{-1} to the C-C skeletal stretching modes. The asymmetric

and symmetric stretching modes of $(CH_3)_4N^+$ are assigned to the bands located at 967 and 760 cm^{-1}. Similar maxima can be detected for the surfactants in the solution, although their intensities are much weaker.

3.2. Formation of porous solid

Figure 2 shows the FT-IR/PAS spectra of the samples, which were periodically taken from the synthesis mixture. The samples were dried and alternatively washed and calcined. It can be observed that silica skeleton is easily formed after ammonium hydroxide introduction to the synthesis mixture containing surfactant molecules and TEOS upon increase of the pH of solution. The results indicate that slight changes of the structure occur during hydrothermal treatment. All samples show stretching vibrations ν_{OH} (Si-O-H) as the broad peak with the centre at around 3440 cm^{-1} connected with the presence o physically adsorbed water. A partial replacement of the templates with water and formation of new hydroxyl groups occur during washing. Samples show triplet located in the range 2800–3000 cm^{-1} assigned to the asymmetric CH_3, CH_2 and symmetric CH_2+CH_3 vibrations of surfactant molecules. Their presence is also evidenced by the bands located at 1970 cm^{-1}, 1870 as C-H vibrations, and 1630 cm^{-1} as R-NH_3^+ vibrations. The removal of the templates by calcination leads to the increase of the amounts of the isolated ≡Si-OH silanol groups, which are visible as sharp peak at about 3740 cm^{-1}, bridging hydroxyl (≡SiOH·OSi) vibrations with the centre at 3650 cm^{-1}, and bending vibration of hydroxyl groups. Bending vibrations of CH_2 and CH_3-N^+ (located at 1460–1490 cm^{-1}) disappear after calcination.

The absorption bands at around 1250–1200 and 1100–1000 cm^{-1} are related to asymmetric stretching vibrations of Si-O-Si bridges, regarded often as “external” and “internal”, respectively [39]. The absorption band at 960–980 cm^{-1} is connected with the stretching vibrations of the Si-OH groups, while the bands at 780–820 cm^{-1}, and 540–580 cm^{-1} are the symmetric stretching vibrations of Si-O-Si bridges. The bands located at 450–460 cm^{-1} are assigned to the Si-O bending vibration [40,41]. The intensity of the vibrations in this region is much lower in the samples before template removal. Slight shift of the Si-O-Si vibrations to higher values can be observed after template removal. This effect can be attributed to the less ordered structure of the silica materials on the early stages of the synthesis and damping of the Si-O-Si vibrations due to the presence of the large organic molecules filling pore system [42].

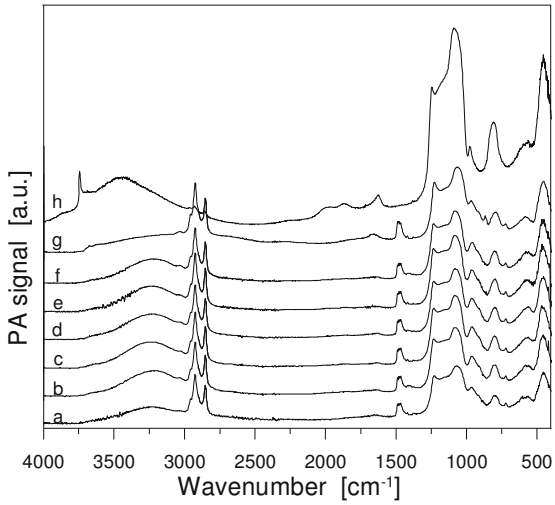

Fig. 2. FT-IR/PAS spectra of the MCM-41 samples taken from the synthesis mixture after different reaction time: a) 10 min., b) 20 min., c) 30 min., d) 40 min., e) 50 min., f) 60 min., g) 60 min. and washing, h) after calcination at 550°C for 6 h.

Similar phenomena are visible in gold containing samples. Figure 3 shows the spectra in the two characteristic regions. An introduction of gold in the initial stage of the synthesis has a weak influence on the surface and framework vibrations. In contrast to the results of the FT-IR studies of gold nanoparticles capped with similar cationic surfactant in water performed by El-Sayed [43], the location of the bands of hydroxyl, amine and hydrocarbons groups incorporated in the pores of MCM-41 and Au-MCM-41 materials is almost the same. This discrepancy can be connected with low concentration of gold in the studied samples. Typical vibrations of the isolated and bridging hydroxyl groups are visible after calcintaion.

Although bending vibration of amine species CH_xN^+ located in the range 1500–1400 cm^{-1} in the samples before calcination are not visible, all samples show the traces of hydrocarbons. Weaker intensity of these vibrations may indicate the enhancement of the removal caused by the presence of gold. Similar phenomena were observed for the MCM-41 materials, based on the octadecyltrimethyl ammonium bromide surfactant. However the intensity of the vibrations of the remaining species were much lower than in the MCM-41 materials, indicating that the removal of the surfactants depends on the pore diameter of the materials. The samples containing gold show slightly lower intensities of the hydroxyl and framework vibrations, which could be related to a partial bonding of hydroxyl surface groups with gold species and less ordered structure of materials.

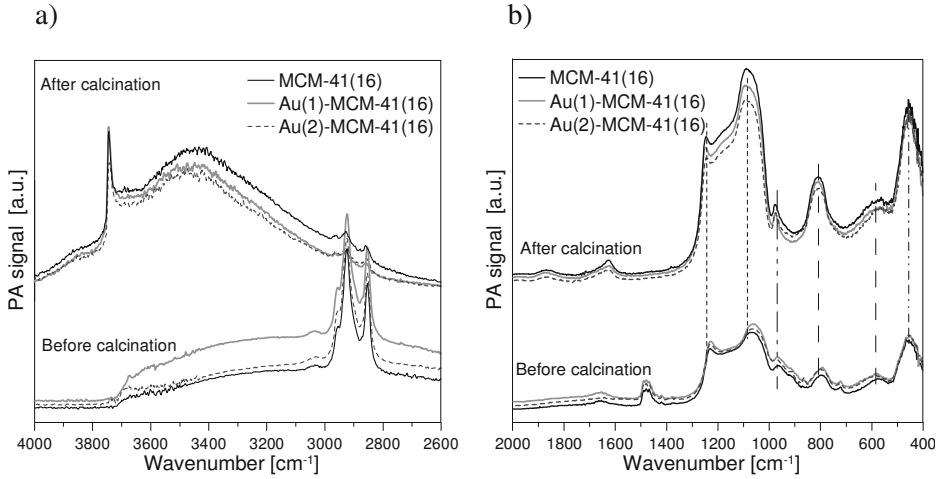

Fig. 3. FT-IR/PAS spectra: a) high-wavenumber region, b) low-wavenumber region.

3.3. Template removal

Figure 4 shows thermal decomposition of the templates in the samples. Weakly bounded water molecules (m/e = 18) and carbon dioxide (m/e = 44) are desorbed in the first stage of the surfactant removal. The evolution of water is also observed at higher temperatures. The maxima in the range 200–250°C are attributed to the transformation of silica skeleton [45]. The presence of trimethyl amine (m/e = 58) is observed in the range 150–300°C. It results from Hofamann elimination of hexadecyltrimethylammonium cation and the formation of unsaturated hydrocarbons [41,42]. The position of this peak is not strongly influenced by gold. Small peak, which occurs for MCM-41 materials at 350°C may indicate the presence of some structural hindrances. However the shift of the small peak to higher temperatures in gold containing materials can be ascribed to the different structural properties, but also to the interaction of amine groups with gold species. Long chains of unsaturated hydrocarbons are eliminated at higher temperatures due to high boiling point and geometrical hindrances by desorption and decomposition or oxidation, which lead to the consumption of oxygen (m/e = 32) and production of carbon oxides (m/e = 28, 44), water (m/e=18), nitrogen oxides (m/e = 30), and heavy oxygenated hydrocarbon compounds. The presence of gold in the MCM-41 materials shifts the oxidation reactions to lower temperatures. The maxima of oxygen consumption, production of CO_2 and H_2O occurs nearly at the same temperatures as the temperatures of trimethylamine formation. The irregular shape of oxygen consumption indicates complex reaction schemes. The intensity of the first negative peak of O_2 is partially related to gold content. Moreover the extent of

the oxidation reaction of hydrocarbons chains at high temperatures increases with an increase of gold content. Similar phenomena we have observed for MCM-41(18) samples. This effect can be explained by the catalytic properties of gold. Similar enhancement of template removal was observed for platinum containing MCM-41 materials [46].

The results show that the presence of gold does not strongly influence the stability of the C-N bonds in the surfactant molecules; however gold enhances the oxidation of the "as-formed" hydrocarbon species. Decomposition of the surfactants to the amines and unsaturated hydrocarbons is an endothermic reaction, while the oxidation reactions are highly exothermic. The intensification of oxidation reactions may disturb the silica skeleton structure and enhance diffusion of gold species confined in the pores to large crystallites. The rate of such processes can be related to the initial gold dispersion. The presence of highly dispersed, small gold species increases the catalytic effect, and as results, may increase a local temperature, leading to increase of the crystallites diffusion effects. The observed phenomena of the surfactant decomposition reveal interesting properties of gold modified silica mesoporous materials as sorbents for N-containing organic compounds, and active catalysts for removal of hydrocarbons in the oxidation reactions at elevated temperatures. Such properties seems to be promising for different applications, e.g. for odour compounds removal.

3.4. Morphology and porous structure

The condensation of silica in the presence of surfactant molecules leads to the formation of the materials with uniform pore arrangement and large surface area, extending 1000 m^2/g. The properties of calcined silica materials modified with gold are presented in the Table 1. The BET surface area, pore volume and pore diameter indicate formation of the materials with mesoporous structure.

Tab. 1. Composition, surface area, pore volume and pore width of the samples.

Sample	Au (wt. %)	S_{BET} (m^2/g)	V (cm^3/g)	w_d (nm)
MCM-41(16)	0	1075	1.1	4.2
Au(1)/MCM-41[16)	0.80	971	0.91	3.8
Au(2)/MCM-41[16)	1.38	1030	1.05	3.7
MCM-41(18)	0	980	1.92	4.9
Au(1)/MCM-41(18)	0.57	956	1.41	4.4

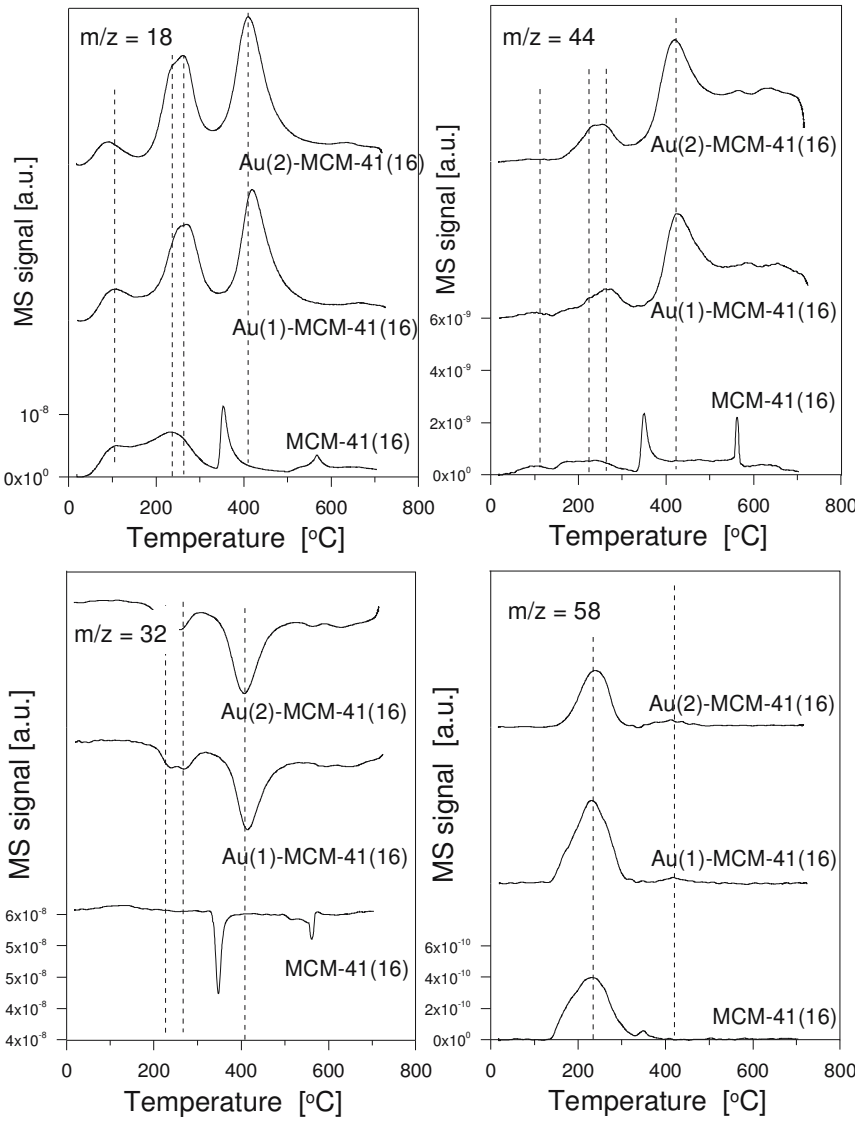

Fig. 4. Temperature programmed decomposition of the templates.

Figure 5 shows the nitrogen adsorption/desorption isotherms. The shape of the curves for pure silica and modified materials reveals the presence of mesopores. The position of the step on the isotherms indicates that the diameter of pores is determined by the chain length of surfactants. The increase of the adsorption at high relative pressures can be related to structural disruption and the presence of large pores between the grains of silica materials.

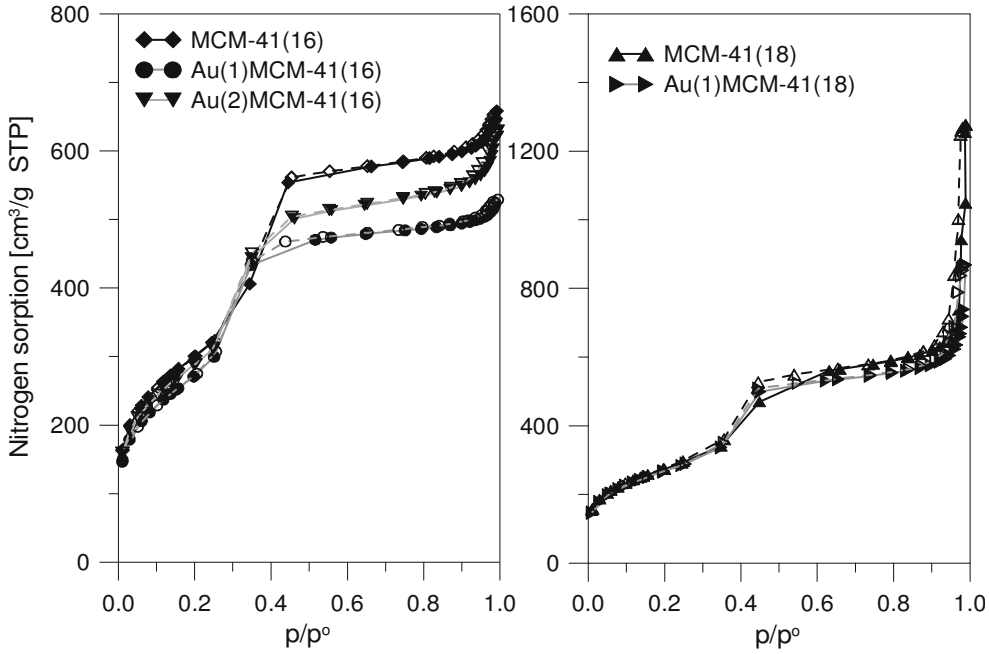

Fig. 5. Nitrogen adsorption/desorption isotherms.

Atomic force microscopy studies show that thensamples contain large rounded particles with the average size of 400 nm, which are surrounded by small particles with less regular shape and size. AFM topographical image show the nonuniformity of the surface of the Au(1)-MCM-41(16) particle (Figure 6).

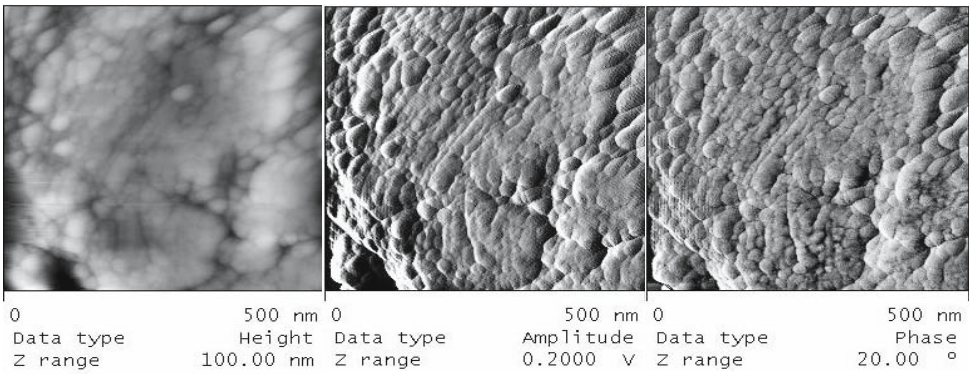

Fig. 6. AFM images of Au(1)-MCM-41 sample; a) topographical, b) amplitude and c) phase mode.

The complex nature of the surface is well visible on the amplitude and phase images. In the phase mode imaging the cantilever oscillations are damped due to interaction with the surface of the sample. The measured phase shift of the oscillations is related to the changes of mechanical properties or viscoelasticity of materials. Detailed analysis of this image could reveal the presence of very small irregularities, related to the entrances of the channels in the grains.

3.5. The nature of gold species

The ordered mesoporous structure is well visible in the TEM images. The results obtained for Au(1)-MCM-41 sample are presented in the Figure 7. The sample contains rounded grains of silica particles with various size and amorphous phase. The materials exhibit the ordering clearly seen in the Figure 7b. An example of gold particle with the size of 3.2 nm is marked with an arrow in the Figure 7c. Slightly different arrangement of pores is observed for Au(2)-MCM-41 sample (Figure 8). FFT (Fast Fourier Transform) pattern of the image presented in the Figure 8b contains well developed spots corresponding to the periodicity of 3.55 nm, close to (100) of MCM-41 (Figure 8c). TEM micrographs of the sample containing large amounts of gold show rounded and elongated particles with the size 5–15 nm distributed over the support. The size of the particles is larger than the size of the channels. However some small spots, with the size corresponding to the pore width, or even smaller, can be distinguished.

Figure 9 shows XRD curves at low-angle diffraction region. The MCM-41 structure is characterized by four peaks, with a very strong peak at about 2θ angle corresponding to (100) reflection, and three weaker peaks at the higher angles assigned to (110), (200), (210) reflections, respectively. The dashed curves in the Figures 9a and 9b correspond to the materials containing surfactant molecules. An increase of the intensity of the peaks after calcination indicates the increase of arrangement of pores. Small shift of the position of the peaks to higher angles, which is observed for all samples, evidences shrinkage of the pores. It is interesting that the extent of this effect is higher for gold containing materials.

In the case of the samples prepared with surfactant of longer alkyl chain length, the position of the (100) reflection occurs at slightly lower values. Similar effect has been often observed for pure and modified silica materials, and ascribed to the formation of larger pores. The obtained results indicate that introduction of the small amounts of gold does not distort structural properties. However an increase of the amounts of gold may change the ordering. Upon addition of ammonia to the solution containing surfactant molecules and TEOS we have observed formation of white gel. The colour of the samples turned to pink or red after drying at elevated temperature. We noted very slight changes of

the colour of the uncalcined samples stored in the translucent glass pot during several weeks.

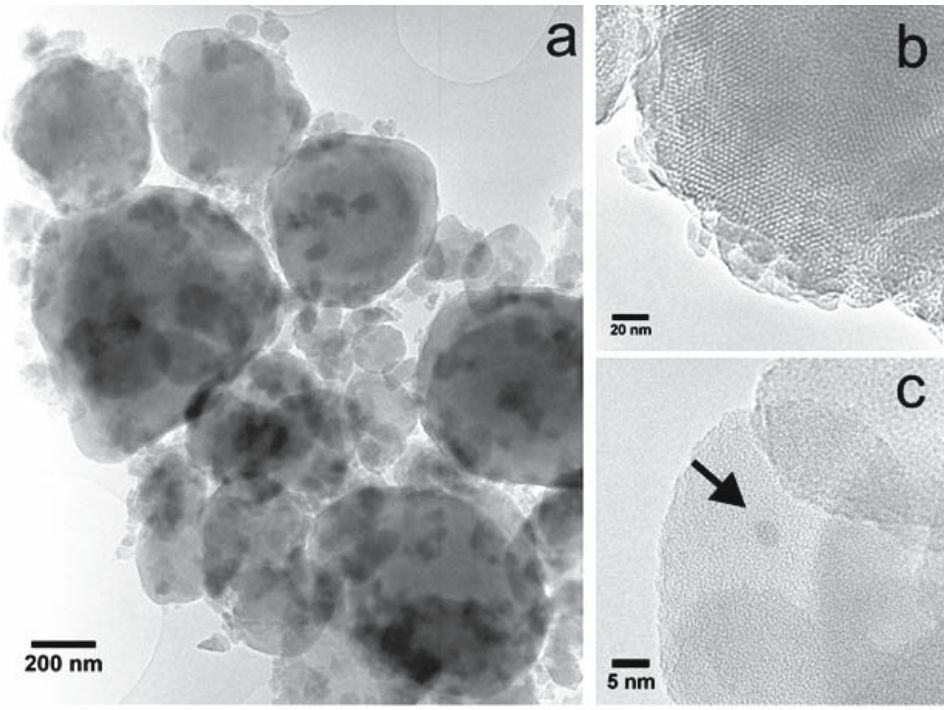

Fig. 7. TEM results for Au(1)-MCM41(16) sample: a) general view, b) high resolution image, c) gold particle.

Figure 10 shows UV-VIS spectra of the selected samples.Studies indicate the coexistence of different forms of gold species in the dried and calcined samples. Well distinguishable absorption bands are located at 255, 330, and 530 nm, respectively. Low-wavelength maxima are ascribed to the presence of Au^{+} cations (I), the region 280–350 nm is considered as indication of $(Au)_n^{\Delta+}$ gold clusters (II), while the band above 500 nm is attributed to gold nanoparticles of different size (III) [47] An increase of gold contents leads to increase of signal intensity. One can observe that the ratio of the intensities of the form (I)/(III) is slightly higher for Au(1)-MCM-41(16) than for Au(2)-MCM-41(16) sample. The position of the maximum of the form (III) of gold species for Au(2)-MCM-41(18) is slightly shifted to higher values, and the ratio of the intensities (I)/(III) is the largest among presented samples. It is visible strong increase of the intensity of the absorbance of the small gold clusters and nanoparticles for all

samples after calcination. Moreover the position of the peaks of the form (III) of gold species moves to lover values of λ. The highest ratio of the signal intensity of the form (II)/(III) can be detected for Au(2)-MCM-41(18) sample, while the lowest one is recorded for Au(1)-MCM-41(16), respectively.

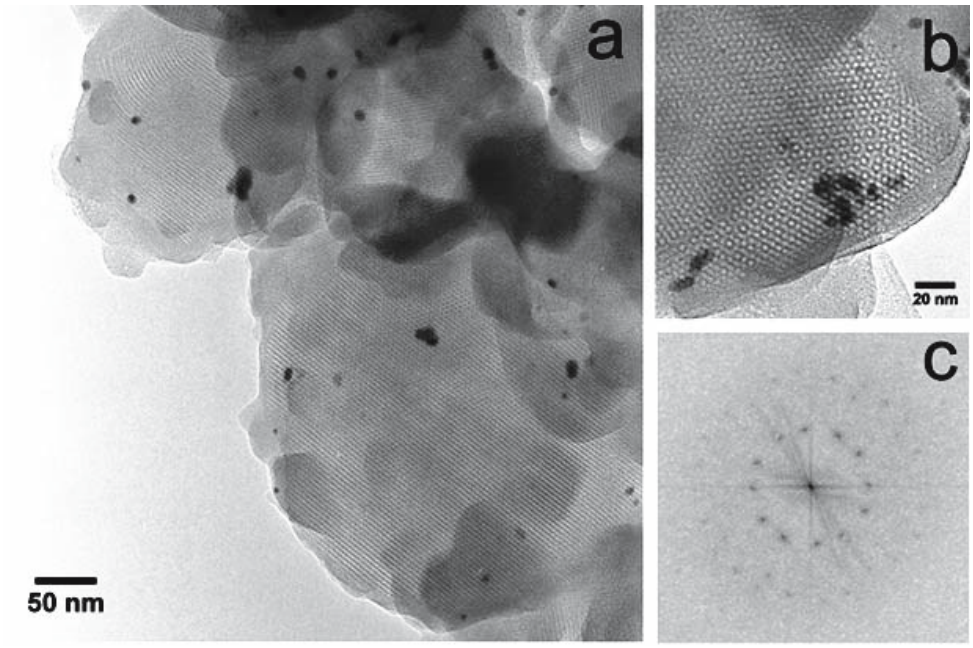

Fig. 8. TEM results for Au(2)-MCM41(16) sample: a) general view, b) high resolution image, c) FFT pattern.

Upon addition of ammonia to the solution containing surfactant molecules and TEOS we have observed formation of white gel. The colour of the samples turned to pink or red after drying at elevated temperature. We noted very slight changes of the colour of the uncalcined samples stored in the translucent glass pot during several weeks. Figure 10 shows UV-VIS spectra of the selected samples. Studies indicate the coexistence of different forms of gold species in the dried and calcined samples. Well distinguishable absorption bands are located at 255, 330, and 530 nm, respectively. Low-wavelength maxima are ascribed to the presence of Au^{+} cations (I), the region 280–350 nm is considered as indication of $(Au)_n^{\Delta+}$ gold clusters (II), while the band above 500 nm is attributed to gold nanoparticles of different size (III) [47] An increase of gold contents leads to increase of signal intensity. One can observe that the ratio of the intensities of the form (I)/(III) is slightly higher for Au(1)-MCM-41(16) than

for Au(2)-MCM-41(16) sample. The position of the maximum of the form (III) of gold species for Au(2)-MCM-41(18) is slightly shifted to higher values, and the ratio of the intensities (I)/(III) is the largest among presented samples. It is visible strong increase of the intensity of the absorbance of the small gold clusters and nanoparticles for all samples after calcination. Moreover the position of the peaks of the form (III) of gold species moves to lover values of λ.

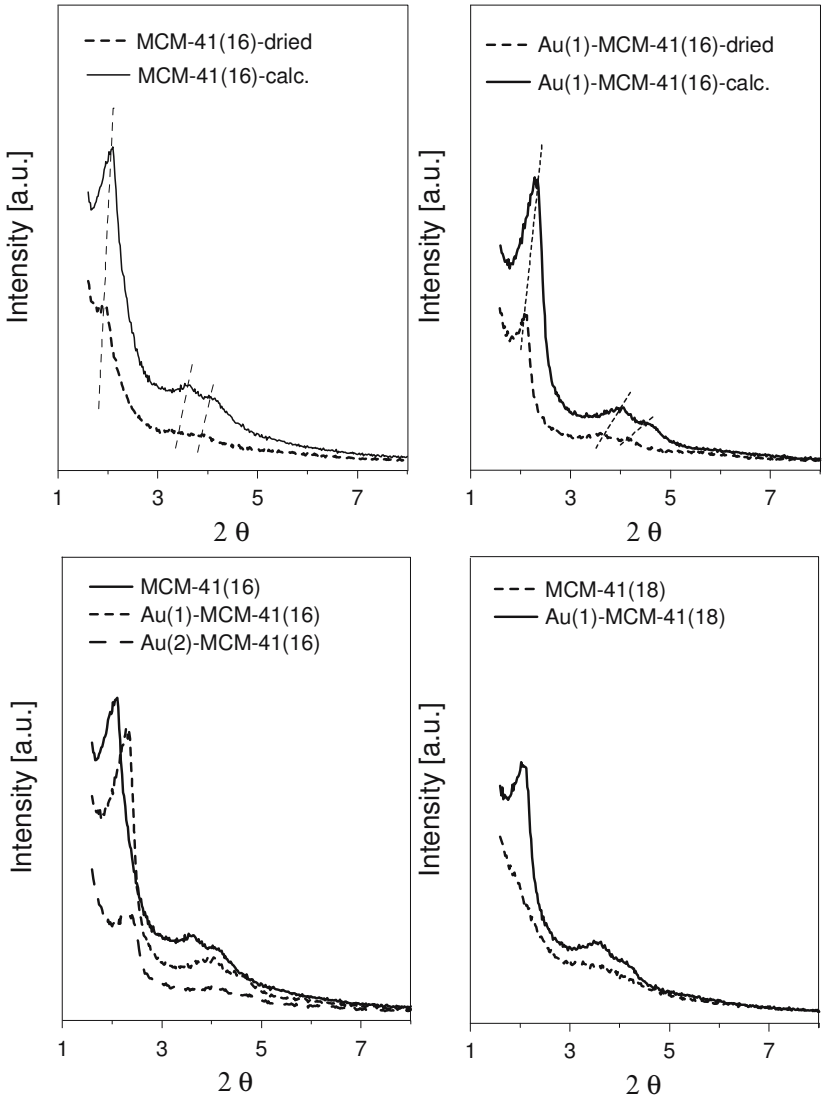

Fig. 9. XRD curves of the samples before and after calcination.

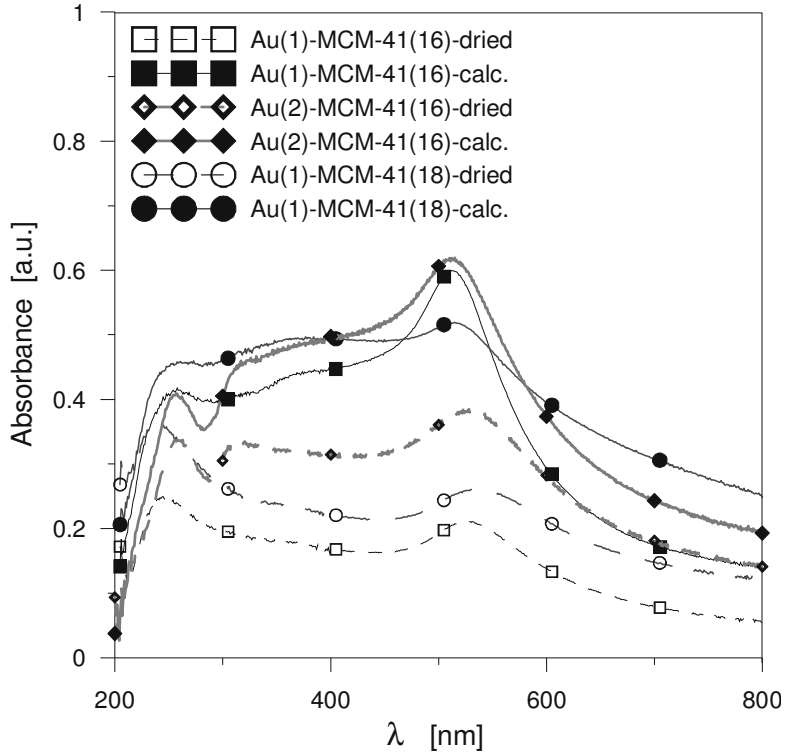

Fig. 10. UV-VIS spectra of the Au-MCM-41 samples: dashed lines – before calcination, solid lines – after calcination.

The highest ratio of the signal intensity of the form (II)/(III) can be detected for Au(2)-MCM-41(18) sample, while the lowest one is recorded for Au(1)-MCM-41(16), respectively.

XRD studies (Figure 11) confirm the presence of relatively small metallic gold species in the dried samples and reveal the changes of the size of the crystallites during calcination. Before high temperature treatment, the Au(1)MCM-41(16) sample show weak peaks, which correspond to the Au(100), Au(200), Au(220) and Au(311) reflections, respectively.

The size of gold crystallites strongly increases during calcination, which is manifested in sharpening of XRD peaks. The discrepancy between XRD and TEM results obtained for Au(1)-MCM-41(16) sample can be connected with nonuniform distribution of the large gold crystallites. The changes of the size of gold species are also visible for Au(2)MCM-41(16) sample; however the effect of the enlargement of gold crystallites is much weaker. Similar shape of the peaks is observed for Au(1)MCM-41(18) sample.

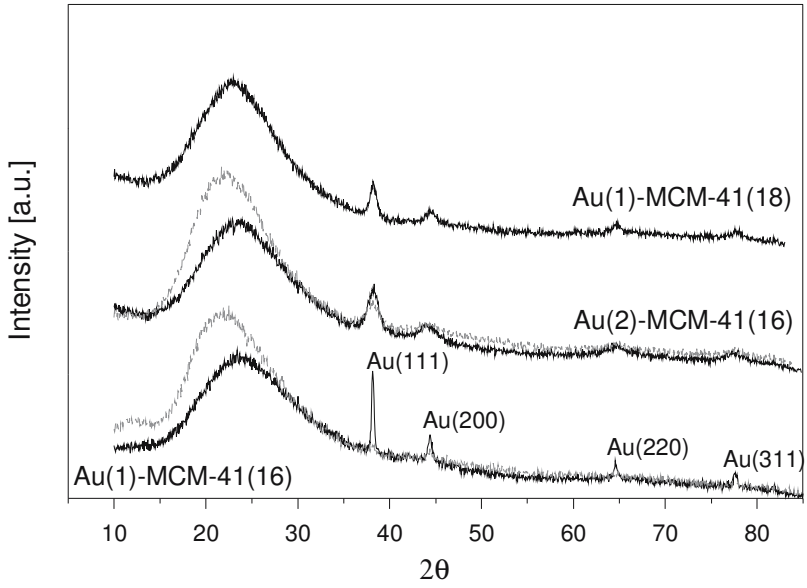

Fig. 11. XRD curves of the selected samples: after drying – grey dashed lines, after calcination – solid lines.

4. CONCLUSIONS

Studies evidenced the changes of the nature of gold species and the properties of silica mesoporous materials on the different preparation stages. Partial hydrolysis of $[AuCl_4]^-$ complex was observed in the dilute solution used for the synthesis. An introduction of cationic surfactants containing bromide ions led to exchange of -Cl with -Br groups. Development of Si-O-Si linkages and simultaneous formation of gold species were observed upon introduction of ammonium hydroxide to the solution containing silica source. A growth of gold species was hindered due to the presence of surfactant molecules. Studies showed that gold species changed the mechanism of template removal. Although the influence of gold on the rapture of C-N bonds in the surfactant molecules was not strongly manifested, the presence of gold enhanced removal of hydrocarbons species formed during elimination reaction, via the oxidation processes. It was demonstrated that the calcination stage may strongly influence the size of gold crystallites. The shape and the size of gold species were identified by the TEM and UV-VIS spectroscopy. Porous structure of the materials was elucidated from the nitrogen adsorption/desorption, XRD and microscopy studies. It was observed that the ordering of pores was not strongly distorted by the introduction of the small amounts of gold. XRD, Raman and UV-VIS spectroscopy studies

revealed the changes of the nature of gold species in the synthesis solution and solid samples.

Acknowledgement. This work was supported by the Polish Ministry of Science and Higher Education as research project No. 3T09B11429.

5. REFERENCES

[1] J. S. Beck, J. C. Vartuli, W. J. Roth, M. E. Leonowicz, C. T. Kresge, K. D. Schmitt, C. T.-W. Chu, D. H. Olson, E. W. Sheppard, S. B. McCullen, J. B. Higgins, J. L. Schlenker, *J. Am. Chem. Soc.*, 114, 10834 (1992).
[2] T. Yanagisawa, T. Shimizu, K. Kuroda, C. Kato, *Bull. Chem. Soc. Jpn*. 63, 988 (1990).
[3] A. Taguchi, F. Schüth, *Micropor. Mesopor. Mater*. 77, 1 (2005).
[4] S. Biz, M. L. Occelli, *Catal. Rev.-Sci. Eng.* 40, 329 (1998).
[5] D.T. On, D. Desplantier-Giscard, C. Danumah, S. Kaliaguine, *Appl. Catal. A Gen*., 222, 299 (2001).
[6] C. W. Corti, R. J Holliday, *Gold Bull.*, 37, 1 (2004).
[7] D. Pissuwan, S. M. Valenzuela, M. B. Cortie, *Trends Biotechn.*, 24, 62 (2006).
[8] E. R. T. Tiekink, *Crit. Rev. Oncol. Hemat.,* 42, 225 (2002).
[9] M. Haruta, T. Kobayashi, H. Sano, N. Yamada, *Chem. Lett*., 2 405 (1987).
[10] M. Haruta, S. Tsubota, T. Kobayashi, H. Kageyama, M. J. Genet, B. Delmon*, J. Catal.*, 144, 175 (1993).
[11] G. J. Hutchings, *Catal. Today,* 72, 11 (2001).
[12] C. W. Corti, R. J. Holliday, D. T. Thompson, *Appl. Catal. A: Gen*., 291, 253 (2005).
[13] G. C. Bond, C. Louis, D. T. Thompson, *Catalysis by gold*, Imperial College Press, London, p. 1, 2006.
[14] P. Claus, *Appl. Catal. A: Gen.*, 29, 222 (2005).
[15] I. Sobczak, A. Kusior, J. Grams, M. Ziolek, *J. Catal*., 245, 259 (2007).
[16] H. Zhu, C. Liang, W. Yan, S.H. Overbury, S. Dai, *J. Phys. Chem. B,* 110, 10842 (2006).
[17] K. Zhu, J. Hu, R. Richards, *Catal. Lett.,* 100, 195 (2005).
[18] Y. S. Chi, H. P. Lin, C. Y. Mou, *Appl. Catal. A: Gen.,* 284, 199 (2006).
[19] J. P. Brunelle, *Pure Appl. Chem.,* 50, 121 (1978) 1.
[20] K. J. Chao, M. H. Cheng, Y. F. Ho, P. H. Liu, *Catal. Today*, 97, 49 (2004).
[21] M. T. Bore, H. N. Pham, T. L. Ward, A. K. Datye, *Chem. Comm*., 2620,2004.
[22] E. M. Claesson, A. P. Philipse, *Coll. Surf. A*, 297, 46 (2007).
[23] W. Yan, B. Chen, S. M. Mahurin, E. W. Hagaman, S. Dai, S. H. Overbury, *J. Phys. Chem. B*, 108, 2793 (2004).
[24] M. Okumura, S. Tsubota, M. Haruta, *J. Mol. Catal. A: Chem*., 199, 73 (2003).
[25] C. Aprile, A. Abad, H. Garcia, A. Corma, *J. Mater. Chem*., 15, 4408 (2005).
[26] M. Grün, K.K. Unger, A. Matsumoto, K. Tsutsumi, *Characterization of Porous Solids IV*, B. McEnaney, J. T. Mays, J. Rouquerol, F. Rodriguez-Reinoso, K. S. W. Sing. K. K. Unger (Eds.), The Royal Society of Chemistry, p. 81, 1997.
[27] S. J. Gregg, K. S. W. Sing, *Adsorption, Surface Area and Porosity*, Academic Press, London, 1982.
[28] M. Kruk, M. Jaroniec; A. Sayari, *J. Phys. Chem. B*, 101, 583 (1997).
[29] W. Rasband, ImageJ, U.S. National Institutes of Health, Bethesda, Maryland, USA, http://rsb.info.nih.gov/ij/, 1997-2005.
[30] M. Lindén, S. Schacht, F. Schücht, A. Steel, K. K. Unger, *J. Por. Mater*. 5, 177 (1998).

[31] S. A. Cotton, *Chemistry of precious metals*, Blackie Academic & Professional, London pp. 301-302, 1997.
[32] P. J. Murphy, M. S. Lagrange, *Geochim. Cosm. Acta*, 62, 3515 (1998).
[33] R. Zanella, L. Delannoy, C. Louis, *Appl. Catal. A: Gen*., 291, 62 (2005).
[34] J. Goworek, A. Kierys, R. Kusak, *Micropor. Mesopor. Mater*., 98, 247 (2007)
[35] J. Perez-Justene, I. Pasttorioza-Santos, L. M. Liz-Marzan, P. Mulvaney, Coord. *Chem. Rev.*, 249, 1870 (2005).
[36] S. Guo, E. Wang, *J. Coll. Interface Sci.*, 315 795 (2007).
[37] H. Omrani, R. Mercier, C. Sourisseau, *Spectrochim. Acta A*, 55, 1411 (1999).
[38] J. Zheng,W. Huang, S. Chen, Z. Niu, Z. Li, *Electrochem. Comm*., 8 600 (2006).
[39] V. L. Zholobenko, S. H. Holmes, C. S. Cundy, J. Dwyer, *Micropor. Mesopor. Mater.*, 11, 83 (1997).
[40] R. K. Rana, R. Viswanathan, *Catal. Lett*., 52, 25 (1998).
[41] J. Ryczkowski, J. Goworek, W. Gac, S. Pasieczna, T. Borowiecki, *Thermochim. Acta*, 432, 2 (2005).
[42] D. C. Calabro, E. W. Valyocsik, F. X. Ryan, *Micropor. Mater*., 7, 243 (1996).
[43] B. Nikoobakht, M. A. El-Sayed, *Langmuir*, 17, 6368 (2001).
[44] F. Kleitz, W. Schmidt, F. Schuth, *Micropor. Mesopor. Mater*., 44-45, 95 (2001).
[45] X. S. Zhao, C. Q. Lu, A. K. Whittaker, G. J. Millar, H. Y. Zhu, *J. Phys. Chem. B*, 101, 6525 (1997).
[46] P. Krawiec, E. Kockrick, P. Simon, G. Auffermann, S. Kaskel, *Chem. Mater.*, 18, 2663 (2006).
[47] J. L. Margitfalvi,. A. Fási, M. Hegedus, F. Lónyi, S. Göbölös, N. Bogdanchikova, *Catal. Today*, 72, 157 (2002).

CURRICULA VITAE

Wojciech Gac. Born in Poland in 1967. He was graduated from Maria Curie-Skłodowska University Lublin in 1992. Received his Ph.D. in chemistry (1996) from the UMCS. His activity is focused on the preparation and characterisation of the catalysts and nanostructured materials for production and utilisation of hydrogen, CO oxidation, methane combustion, NO_x and volatile compounds abatement. Scientific coordinator and participant of research projects of the Ministry of Science and Higher Education of Poland, and scientific cooperation joint projects (Greece, Hungary, Ukraine, Spain).

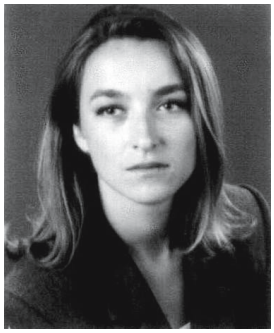

Sylwia Pasieczna-Patkowska. Born in Poland in 1974. Graduated from the University of Maria Curie-Skłodowska (UMCS) in Lublin (1998). Received his Ph.D. (2006) in physical chemistry from the University of Maria Curie-Skłodowska (UMCS) in Lublin. Since 2007 he is an adiunct at UMCS. Member of Polish Chemical Society (since 1998), Polish Catalysis Club (since 1998).